ISBN: 978-628-96613-3-0. ISSN: 2414-6390. Digital Object Identifier: https://dx.doi.org/10.18687/LACCEI2026.1.1.2582

Conceptual Design of a Low-Cost Extrusion-Driven Injection Molding Device for Polymeric Materials

Franklin Moset Vega[1], Antonio Jaén-Ortega[1,3], Maria De Los Ángeles Ortega-Del-Rosario[1,2,3]
[1]Research Group in Design, Manufacturing and Materials (DM+M), School of Mechanical Engineering, Universidad Tecnológica de Panamá, Panama City 0819-07289, Panama, franklin.vega@utp.ac.pa; maria.ortega@utp.ac.pa
[2]Polymer Chemistry and Biomaterials Group, Centre of Macromolecular Chemistry, Department of Organic and Macromolecular Chemistry, Ghent University, Krijgslaan 291 S4, Ghent, Belgium; Antonio.JaenOrtega@UGent.be
[3]Sistema Nacional de Investigación (SNI), Clayton Panama City, Panama

Abstract*– Conventional polymer injection molding achieves high part quality and productivity; however, equipment and tooling costs frequently restrict its use in educational laboratories and early-stage research settings. This study introduces a requirement-driven conceptual design for a low-cost injection molding device that uses readily available filament-extrusion hardware to fabricate ASTM D638 Type I specimens. The methodology translates functional requirements into integrated subsystem decisions for the injection unit, mold unit, and structural frame, supported by first-order flow, thermal, and mechanical analyses. The design process establishes a feasible low-throughput operating window and addresses key risks through targeted solutions: guideline-based venting to minimize gas entrapment, conduction-focused mold heating with cartridge heaters and optional cooling channels for thermal regulation, and a stable clamping and alignment strategy for precise nozzle-to-mold positioning. Sprue and runner alternatives were assessed as coupled variables, with the constant-cylindrical sprue selected as the most robust option for maintaining quality consistency, mitigating defects, and maintaining dimensional stability under laboratory constraints. Material screening and preliminary sizing criteria identified aluminum tooling as suitable for the reference configuration. The resulting framework offers a practical pre-prototyping approach for low-volume comparative testing, educational use, and early laboratory validation, while excluding industrial high-throughput operation from its intended scope.

Keywords*-- Injection molding; Additive manufacturing; FDM extrusion; Conceptual design; Polymer processing.

I. Introduction

Recent years have seen increased demand for sustainable, lightweight, and cost-effective solutions in industries that rely on polymeric materials, including sports, automotive, and aerospace [1], [2]. This demand has highlighted the need for manufacturing methods capable of producing functional thermoplastic parts with reliable performance, while remaining accessible for product development, testing, and low-volume production [3], [4], [5], [6], [7]. In response, material-extrusion additive manufacturing (AM) has gained widespread adoption due to its ability to rapidly fabricate parts from digital models, accommodate complex geometries, and lower barriers to prototyping. The most common implementation involves melting thermoplastic filaments and depositing them through an extrusion system, with the toolhead and build platform moving along three axes to construct the part layer by layer [8], [9], [10], [11], [12].

Despite its accessibility and geometric freedom, material-extrusion AM faces well-known limitations when parts must be mechanically representative. The layer-by-layer deposition process introduces interfaces that can compromise structural integrity and lead to anisotropy, which is particularly problematic when tensile performance and repeatability are required for engineering evaluation. Additionally, achieving consistent quality often depends on careful control of process parameters, material condition, and geometry-dependent printing strategies. These constraints can make it difficult to use printed parts as direct substitutes for injection-molded components when the objective is to validate performance under standardized testing and realistic loading conditions [13], [14], [15], [16], [17], [18], [19]

Injection molding remains one of the most effective methods for producing thermoplastic parts with high repeatability, superior surface finish, and properties that closely approximate isotropic bulk behavior. However, its application in prototyping and low-volume production is often constrained by the high cost of tooling, specialized equipment requirements, and operational complexity [20], [21]. Tooling design and fabrication require specialized expertise, and even for small parts, the mold design process entails technical trade-offs regarding filling, cooling, part ejection, and dimensional stability. Consequently, injection molding is often impractical for educational laboratories, early-stage product development, and settings in which only a limited number of test specimens or functional prototypes are required [22], [23], [24].

AM can support injection molding by reducing tooling lead time and enabling rapid fabrication of mold inserts, including features that are difficult to machine with conventional methods. These directions suggest that, rather than treating the two technologies as competing alternatives, it is valuable to identify complementarities that enhance feasibility for low-volume applications. In particular, there is an opportunity to rethink prototyping workflows by combining the accessibility of material-extrusion hardware and the part consolidation benefits of molding logic, with the goal of producing testable polymer parts at lower cost and with improved performance relative to layer-based prints [22], [25], [26], [27].

This study employs an exploratory and analytical approach to examine whether opportunities exist to enhance the profitability and performance of prototyping processes for polymer part manufacturing. This objective motivates research that assesses the technical feasibility of a compact molding device concept that leverages AM strategies and incorporates injection-molding principles.

The concept leverages widely available extrusion components and filament feedstock to create a small-scale injection mechanism, applying mold design logic to produce molded parts suitable for engineering evaluation. To provide a practical context, the study focuses on a standardized tensile specimen geometry, specifically the ASTM D638 Type I format [28], as the target mold cavity and reference for subsequent design decisions.

The scope is limited to conceptual and preliminary design, supported by structured analysis, and does not include the fabrication of a physical prototype at this stage. The methodology integrates comparative analysis of both manufacturing routes, identification of key variables linking process choices to expected part performance, functional decomposition into subsystems, and first-order feasibility calculations for volumetric flow, filling time, and pressure requirements. Furthermore, the study aligns with broader sustainability objectives related to industrial infrastructure and responsible production, emphasizing accessibility, efficiency, and improved decision-making in prototyping.

This paper offers three primary contributions. First, it presents a comparative analysis of material-extrusion AM and injection molding to inform low-volume prototyping decisions regarding performance, accessibility, and implementation constraints. Second, it introduces a structured conceptual architecture for a compact molding device, decomposed into injection, mold, and structural units to facilitate coherent integration of subsystems. Third, it provides a preliminary feasibility assessment based on volumetric flow, filling time, and pressure calculations, establishing viability parameters for the proposed concept at the conceptual stage.

II. METHODOLOGY

This work employed an exploratory, analytical, and design-oriented methodology to conceptually develop a low-cost polymer molding device inspired by material-extrusion AM hardware and injection-molding logic. The study was guided by the following research question: *Can a conceptually designed device, based on material-extrusion components and injection-molding principles, improve the feasibility of polymer prototyping in terms of technical performance and accessibility?* To address this question, the study adopted a feasibility-driven design objective centered on defining an operational window in which an extrusion-based injection concept can reliably fill a standardized cavity with acceptable thermal stability and sealing, using readily available components and a low-cost feedstock. The methodological workflow was organized in five stages.

A. State-of-the-art review
A structured review of scientific and technical literature was conducted to establish current capabilities, limitations, and reported integration approaches between fused deposition modeling and injection molding, with emphasis on process behavior, material response, and design constraints relevant to conceptual device development.

B. Comparative technical analysis (AM vs. injection molding)
A comparative analysis was developed to contrast the two manufacturing routes and identify key trade-offs for low-cost prototyping, including productivity, geometric flexibility, expected mechanical performance, and implementation complexity.

C. Parameter-to-property mapping
Critical variables were identified and systematized across three domains: process parameters, material-related parameters, and geometry-related parameters. Their relationships with expected part performance were mapped to support criterion-based decisions for material selection, process definition, and functional requirements of the proposed device.

D. Functional decomposition and conceptual design
The proposed system was translated into a functional architecture and developed through subsystem-level conceptual design. Requirements were defined, and the main functions were decomposed to ensure coherent integration of subsystems. The device was organized into three main units: (i) injection unit, (ii) mold unit, and (iii) structural support unit.

E. Preliminary feasibility assessment
A first-order engineering feasibility assessment was performed using pressure, volumetric flow, and filling-time calculations to verify conceptual viability and define operational limits for the proposed injection approach using extrusion components. The scope of this work is limited to conceptual and preliminary design; therefore, no physical prototype was fabricated at this stage. The pressure and filling analysis was formulated using a compact set of first-order governing equations. The maximum admissible extrusion pressure was bounded by the filament critical pressure criterion:

$$P_{cr} = \frac{\pi^2 E d_f^2}{16 L_f^2} \quad (1)$$

where E, d_f, and L_f denote filament elastic modulus, filament diameter, and unsupported filament length, respectively. Melt flow in the HotEnd was modeled as non-Newtonian using a power-law representation:

$$\dot{\gamma} = \phi\, \tau^m. \quad (2)$$

The total pressure drop across the HotEnd was computed as the sum of three geometric zones:

$$\Delta P = \Delta P_1 + \Delta P_2 + \Delta P_3 \quad (3)$$

and outlet pressure was obtained from:

$$P_{out} = P_{in} - \Delta P. \quad (4)$$

Finally, cavity filling time was estimated through volumetric continuity:

$$t_{fill} = \frac{V_c}{Q}. \quad (5)$$

As a result, the study presents a concept-level device proposal, supported by a literature-based comparison, functional decomposition, and preliminary calculations that establish viability bounds for future prototyping and experimental validation.

III. Results and Discussion

A. Existing Literature Analysis and Comparative Baseline

A review of the existing literature demonstrates that material-extrusion AM offers high accessibility, low entry costs, and rapid design iteration, making it suitable for early-stage prototyping and laboratory-scale development. However, significant limitations arise when mechanically representative specimens are needed, primarily due to deposition-driven interfaces, anisotropy, and sensitivity to process conditions. These factors can undermine repeatability, surface finish, and consistency of mechanical performance across specimens [14], [15], [16], [17], [19], [29], [30].

In contrast, injection molding is widely regarded as the standard method for producing repeatable thermoplastic parts and standardized test specimens. Controlled cavity filling and solidification typically result in improved part homogeneity, dimensional stability, and reproducibility. However, its adoption in laboratory and low-volume settings is limited by equipment costs, tooling and machining requirements, and operational complexities, such as clamping and thermal management. [20], [22], [23], [24], [26], [31].

These findings establish a practical tradeoff for low-volume prototyping. Material-extrusion platforms are favored for their accessibility and simplified material feeding and melting, while injection molding is preferred for specimen repeatability and improved consolidation. This tradeoff supports the development of a compact approach that uses readily available extrusion-derived components for feeding and melting, combined with injection-molding principles to achieve controlled cavity filling for standardized testing and comparative evaluation. This approach prioritizes specimen consistency over industrial cycle time.

B. Functional Requirements and Design Drivers

To translate the comparative baseline into a requirements-driven device concept, a functional analysis was conducted to formalize the system's functionality and the constraints governing its operation. The outcome of this stage is summarized as a functional tree that links the principal function to life-cycle stages, service functions, and explicit restrictions relevant to assembly, safety, sealing, and thermal stability (see Table I). This functional framing ensures that subsequent design choices are evaluated against traceable, verifiable requirements rather than being driven solely by geometric preference or component availability.

TABLE I
Functional tree of the proposed device, including life-cycle stages, service functions, and design restrictions.

Principal function	Life cycle stage	Service function	Restrictions
F1. Enable molding of standardized specimens using FDM filaments.	Design; Use	F1.1 The mold cavity CAD must accommodate thermoplastic FDM filaments. F1.2 The molding chamber must match the target specimen geometry.	FR1. Dimensions and component locations must be unambiguous for assembly and operation.
F2. Maintain low-cost implementation.	Design; Procurement	F2.1 Components and materials should be widely available. F2.2 Prefer modular parts to reduce tooling and machining needs.	FR2. Materials/components must be safe under intended use (non-toxic and non-reactive).
F3. Provide controlled melt delivery into the cavity.	Use	F3.1 The extrusion-based subsystem must provide stable melting and conveyance. F3.2 Actuation must deliver repeatable volumetric flow during filling.	FR3. Flow must be sustained without premature solidification during long filling times.
F4. Ensure that mold closure and sealing are achieved during injection.	Use	F4.1 The structure must maintain alignment between mold halves/inserts. F4.2 Sealing elements must prevent leakage under pressure.	FR4. No leakage is allowed; deformation must not compromise alignment.
F5. Enable mold temperature control.	Use	F5.1 Integrate heating to keep mold temperature within the processing window. F5.2 Control must be compatible with the selected mold material.	FR5. Temperature must remain within safe limits; overheating must be prevented.
F6. Enable heat removal and part release.	Use; End of cycle	F6.1 Provide cooling to enable demolding and cycle completion.	FR6. Cooling must not induce misalignment; dimensional stability must be maintained.

Based on this functional tree and the design intent, the main design drivers were then prioritized to reflect the intended use case of low-volume prototyping. The highest priority is the successful fabrication of polymer parts using accessible and affordable feedstocks, followed by improved specimen quality relative to material-extrusion limitations, particularly with respect to surface quality and mechanical performance consistency. Cost accessibility relative to conventional injection molding equipment remains a core requirement, while ease of assembly and user-friendly operation support feasibility in laboratory settings. Aesthetics and perceived build quality are treated as secondary but remain relevant attributes for straightforward handling and adoption.

TABLE II
PRIORITIZED DESIGN DRIVERS .

Priority	Design driver
1	Successful fabrication of polymer parts using accessible and affordable feedstock (FDM filaments).
2	Improved part quality relative to material-extrusion AM limitations, particularly surface quality and mechanical performance consistency.
3	Competitive quality-to-cost relationship to ensure overall accessibility versus conventional injection molding equipment.
4	Ease of assembly to reduce fabrication time, energy use, and total design cost.
5	User-friendly operation without the need for extensive specialized training.
6	Adequate aesthetics and perceived build quality for straightforward handling.

Based on functional decomposition and prioritized design drivers, the most relevant criteria were quantified to support traceability from requirements to subsystem decisions. Table III summarizes the targets, flexibility levels, verification approach, and supporting sources used to define the design envelope of the proposed device.

TABLE III
CRITERIA CHARACTERIZATION OF THE PROPOSED DEVICE.

Criterion	Target/specification	Flexibility level	Control/verification	Source
Feedstock dimensions	Filament diameter: 1.75 mm; spool envelope: 20 × 5.3 × 7 cm.	F1	Design review	[32]
Cavity geometry	Standard tensile specimen for polymer testing (ASTM D638 Type I).	F1	Design review	[28]
Mold insulation compatibility	No chemical reactivity between mold material and insulation material (if insulation is required).	F2*	Design review; material screening	Design criterion
Sprue/gate entrance	External entry diameter less than or equal to 5/32 in.	F0	Design review	[33] [34]

*If insulation becomes strictly necessary, the flexibility level may be increased to F1 or F0, depending on the application need.

The results provide a foundation for evaluating subsequent outcomes of the study. Specifically, they support the adoption of modular architecture comprising injection, mold, and structural units; identify temperature control as an essential functional requirement; and validate standardized specimen geometry as a basis for repeatable testing. Consistent with the defined scope, the concept emphasizes specimen consistency and controlled filling behavior rather than industrial productivity.

C. Parameter-to-Property Mapping

Key variables were categorized into three domains to translate the requirements outlined in Tables I–III into engineering implications. Process parameters encompass extrusion and actuation settings that determine melt delivery rate, volumetric flow, and the resulting pressure demand. Material-related parameters describe thermoplastic flow behavior and thermal sensitivity, which influence fillability and the risk of premature solidification during extended filling times. Geometry-related parameters include cavity volume, gate and runner dimensions, and flow-path length, all of which directly affect filling time, pressure losses, and dimensional stability. This framework demonstrates that conceptual feasibility is primarily determined by the interaction among volumetric flow capability, mold thermal control, and the standardized cavity and gate geometry selected for testing. This approach provides direct traceability from the functional criteria to the feasibility bounds discussed in the following section.

D. Architectural Analysis and Conceptual System Architecture

The architectural analysis translated the prioritized functional requirements into a subsystem-based system structure, defining the main modules and their interfaces to ensure coherent integration. The resulting architecture organizes the device into three main subsystems: a Structural Frame, an Injection Unit, and a Mold Unit (Figure 1). This decomposition separates (i) mechanical stability and alignment functions, (ii) melt delivery and actuation functions, and (iii) cavity definition and thermal management functions, respectively. Functional interactions and material-flow pathways were mapped across these subsystems to clarify the dependencies between extrusion-based melt generation, mold filling, and temperature control. The architecture also highlights the central role of the internal mold as the integration node, where the injection unit delivers molten polymer, and the mold unit provides controlled heating and cooling to sustain flow during filling and enable part release.

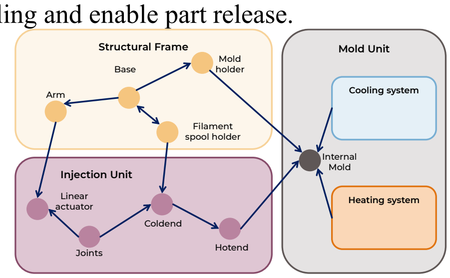

a

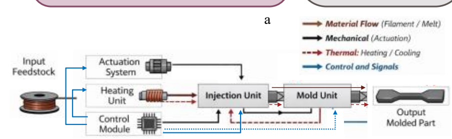

b

Fig. 1 System architecture and functional flow representation of the proposed extrusion-driven injection device. (a) Subsystem-level architectural decomposition showing the three primary units. (b) Functional flow diagram representing material, mechanical, thermal, and control streams across subsystems.

E. Geometric Alternatives for Mold Design and Feasibility of Parting-Plane Selection

A geometric feasibility assessment evaluated the manufacturability of the standardized tensile specimen (ASTM D638 Type I) within a compact extrusion-driven injection system. The analysis considered parting plane definition, mold opening direction, cavity orientation, and the potential for undercut formation.

Figure 2 presents the geometric reasoning process underlying the selection of mold configurations. The evaluation began with a simplified parametric mold block (L × W × H), followed by assessment of specimen orientation relative to the mold opening direction. Two alternative mold variants, designated MV1 and MV2, were examined.

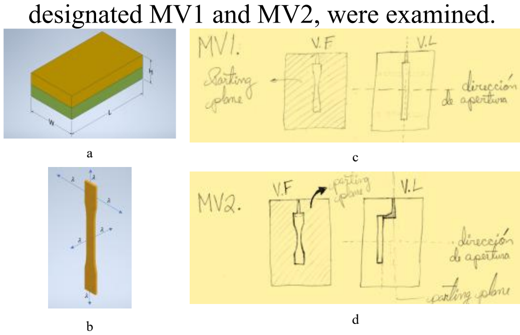

Fig. 2 Geometric feasibility assessment of the proposed mold configuration. (a) Simplified parametric mold block (L, W, H) used to define cavity envelope and parting-plane positioning. (b) Three-dimensional representation of the standardized tensile specimen highlighting principal geometric directions and characteristic dimensions. (c) MV1 configuration: specimen aligned with the mold opening direction and symmetrically divided by a planar parting surface, enabling straightforward demolding. (d) MV2 configuration: rotated specimen orientation relative to the opening direction, illustrating potential demolding complications and increased geometric complexity.

In the first configuration (MV1), the tensile specimen is aligned with the mold opening direction and positioned symmetrically relative to the parting plane. This arrangement enables direct demolding without geometric interference and reduces the risk of undercuts. The planar separation surface is compatible with conventional two-plate mold architecture, facilitating effective sealing and alignment under moderate clamping loads.

In contrast, the second configuration (MV2) features a rotated specimen orientation relative to the opening direction. Although this arrangement is geometrically feasible, it produces non-uniform cavity spacing and increases the risk of geometric locking or asymmetric demolding stresses. Furthermore, the inclined flow path complicates gate positioning and increases sensitivity to melt-front progression during filling.

Based on this comparative assessment, MV1 was selected as the preferred geometric solution due to its compatibility with a planar parting surface, predictable opening kinematics, and reduced geometric complexity. This selection supports the device's low-volume, laboratory-oriented objectives, prioritizing mechanical simplicity, repeatability, and alignment stability over complex multi-part mold architectures.

The selected orientation also facilitates subsequent pressure and filling-time calculations, as detailed in Section IV.E, by ensuring a well-defined cavity volume and a controllable flow compatible with the chosen gate geometry.

F. Preliminary Feasibility Calculations and Viability Bounds

F.1. Process operating window

First-order calculations define the process operating window and conceptual feasibility limits of the proposed extrusion-driven injection configuration. For the selected standardized tensile-specimen cavity, the calculated cavity volume is 8399.631 mm^3 (8.399631 cm^3). At the operating point of 32.56 mm^3/s, the estimated filling time is 258 s (approximately 4.3 min), placing the system in a low-throughput regime and highlighting the need for thermal control to prevent premature solidification during filling.

Pressure calculations indicate an outlet pressure near 7.7 MPa, with minor variation across the evaluated temperature range. This level is consistent with fused-filament extrusion physics, in which the filament acts as a piston that pressurizes the melt through the hot end and nozzle, and the required pressure is governed by melt rheology and flow-path geometry [35], [36]. By comparison, conventional injection molding typically operates at substantially higher pressures, commonly reported to range from 40 to 200 MPa, depending on part and process conditions [31], [37], [38].

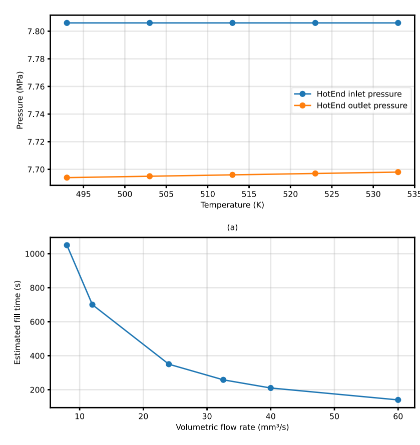

Fig. 3 Operational bounds of the proposed extrusion-driven injection system. (a) Pressure response at the HotEnd inlet and outlet over the evaluated temperature range. (b) Filling-time sensitivity to volumetric flow rate for the selected standardized tensile-specimen cavity, highlighting the trade-off between flow capacity and process duration.

As shown in Figure 3(a), the predicted hot-end inlet pressure remains approximately 7.806 MPa, while outlet pressure stays within about 7.694 to 7.698 MPa over 493 to 533 K, indicating stable pressure behavior under the selected conditions. Figure 3(b) shows that filling time decreases monotonically with increasing volumetric flow rate. However, at the selected operating point, filling remains in the minute-scale range. This contrasts with industrial injection molding, where filling is commonly completed on second-scale cycles, reinforcing that the present configuration is designed for controlled, low-volume prototyping and comparative specimen fabrication rather than high-throughput production [39], [40].

Given this intended use, the manufacturing scope was conservatively capped at 1000 parts. Gate-sizing analysis recommended a 5/32 in entry diameter (about 3.97 mm) as a feasible balance between flow and pressure requirements for the selected cavity. Material screening identified two mold candidates: a 3D-printed polymer and 6061-T651 aluminum. During this process operating window, mold selection was guided by SPI class specifications reported by Kazmer [41], in which Class 101, 102, and 103 molds are associated with production scales of more than 1,000,000, 500,000, and 250,000 cycles, respectively. Given that the present concept is intentionally scoped to approximately 1000 parts, the design is positioned well below the high-volume SPI classes. Therefore, within the current operating constraints (minute-scale filling and sustained thermal demand), the material selection prioritizes thermal stability and dimensional consistency, supporting the selection of Al 6061-T651 as the preferred mold material for the conceptual comparative tool.

F.2. Effect of sprue geometry and runner length

This section presents the rationale for selecting the constant cylindrical sprue as the baseline geometry for the ASTM D638 Type I comparative mold. Analysis of Figure 4(a) demonstrates that the cylindrical sprue consistently achieves higher final quality than the conical alternative across the evaluated runner-length range. For example, at 34 mm, the cylindrical configuration achieves 99.72% quality, compared with 99.56% for the conical; at 5 mm, the values are 99.36% and 99.32%, respectively. Although these differences are quantitatively small, their persistence indicates a systematic advantage for the cylindrical geometry under both limiting conditions.

Figure 4(b) indicates that the sink depth associated with the cylindrical sprue remains close to 0.01 mm for runner lengths between 5 and 30 mm, with a noticeable increase only at 34 mm. This trend suggests greater robustness to variations in runner length within the practical range. Figure 4(c) shows that the conical sprue is associated with increased deflection, while the most favorable deflection (approximately 0.80 mm) is observed under short-runner conditions. Taken together, these findings support the cylindrical configuration with respect to geometric repeatability and surface integrity, although the magnitude of the benefit warrants further examination.

Figure 4(d) corroborates the principal trade-off: volumetric contraction increases with runner length, reaching approximately 5.06% for the cylindrical case and declining to approximately 4.92% at shorter runner lengths. Notably, the greatest disparity between sprue types remains below 5%. This contraction penalty, while measurable, appears comparatively minor when juxtaposed with the observed gains in quality and defect mitigation.

The field maps in Figures 4(f.1) and 4(f.2) (cylindrical sprue, 10 mm runner) align with these trends: contraction is distributed along the specimen body, while sink marks are localized near the sprue-entry transition and remain low in absolute magnitude. These observations support the use of the cylindrical sprue as the reference geometry and suggest that runner length should be considered a secondary tuning variable.

Within the process operating window defined in Section F.1 (approximately 7.7 MPa outlet pressure and minute-scale filling), the primary design objective is to ensure stability and repeatability of specimen quality rather than to maximize throughput. In this context, the cylindrical sprue provides the most favorable balance among competing criteria. However, it is important to recognize that results may differ under alternative operating conditions.

Finally, the diameter-sensitivity analysis supports this selection: after an initial estimate near 5/32 in, a 4.5 mm sprue entry was retained because it reduced both deflection and contraction, maintained sink performance, and resulted in a quality decrease of only about 0.11%, which is considered negligible for the intended application. The constant cylindrical sprue was selected as the final geometry because it improves surface quality and defect robustness (sink and deflection) with only a minor, acceptable increase in volumetric contraction. Nevertheless, further validation in broader contexts is recommended.

F.3. Venting, Thermal Management, and Structural Integration

In closed-cavity injection molding, cavity filling requires the controlled evacuation of gas. Leakage through parting-line interfaces, ejector-pin clearances, or slider interfaces is typically insufficient. For this reason, a dedicated venting system is a mandatory design requirement for molds. Vents are implemented as shallow slots that allow gas release while preventing melt escape, with special emphasis on the last-to-fill region, where inadequate venting can cause air entrapment, short shots, and gas-burn defects. Under high compression, trapped gases may overheat and, in severe cases, damage mold steel. Vent design is parameterized by D_v (vent depth, resin-dependent), L_v (vent length), W_v (vent width), and D_c (post-vent channel depth). The selected values follow established design guidelines [33], [42], as $D_c = 1.00$mm, $L_v = 3.80$mm, $D_v = 0.07$mm, and $W_v = 5.00$mm. These values were held constant across the reference configuration and were used in all subsequent calculations.

For the mold unit, thermal management is defined as a core design function that ensures melt-process stability and part release. The system is configured to heat the mold to the polymer melting temperature during filling and then reduce the temperature for demolding. A conduction-based heating strategy with cylindrical cartridge heaters is adopted as the primary concept, because cartridge heaters provide high heat flux, fit compact cavities, and support integrated thermocouples for closed-loop temperature control. Their geometric flexibility in diameter and cold-section customization also facilitates adaptation to cavity constraints, while appropriate materials and placement enable operation at high temperatures [43]. In this layout, heater cartridges are oriented with their axial direction parallel to the mold width for practical installation and operator accessibility (Figure 5).

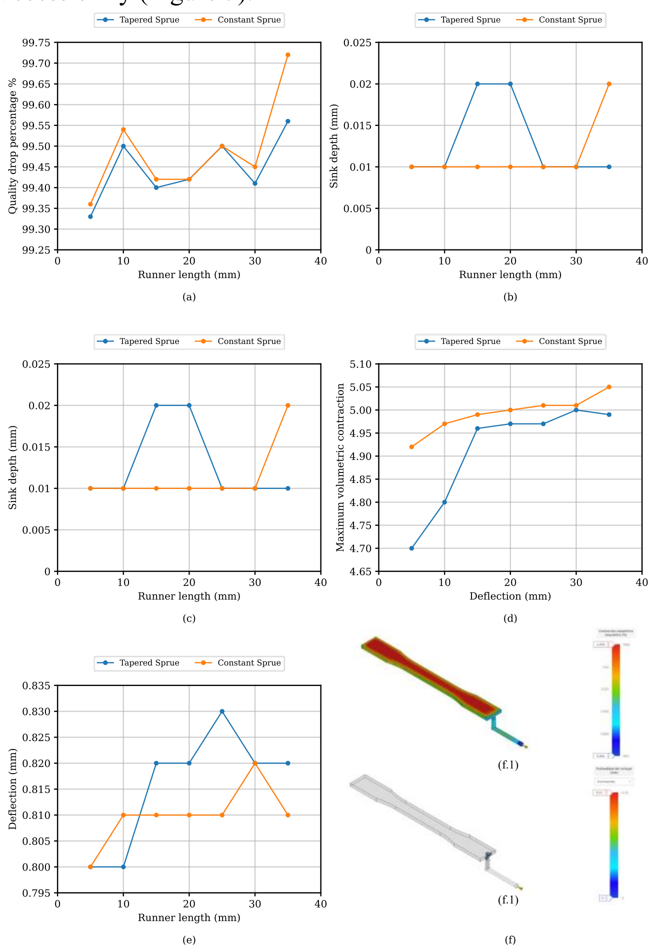

Fig. 4 Effect of sprue geometry and runner length on molding quality indicators for the standardized tensile-specimen cavity. (a) Final quality percentage as a function of runner length. (b) Sink depth versus runner length. (c) An additional sink-depth comparison was used to confirm the same trend under the evaluated design set. (d) Maximum volumetric contraction in relation to deflection. (e) Deflection versus runner length. (f) Spatial fields for the selected baseline condition, performed in ANSYS® (constant cylindrical sprue, 10 mm runner): (f1) volumetric contraction distribution (%) and (f2) sink-depth localization (mm).

Since the mold is intended for comparative research rather than mass production, cycle time is treated as a secondary constraint. Therefore, cooling can be implemented either through predefined water-cooling channels or by natural convection at ambient conditions. When accelerated cooling is required, the channel cross-section and spacing are defined in accordance with the prescribed geometric guidelines. Overall, thermal-line configuration is optimized to achieve two coupled targets: uniform cavity heating to prevent premature solidification and controlled cooling to reduce cycle time while minimizing warpage. Mold closure is achieved using upper and lower fastening bolts, positioned to avoid interference with the thermal circuits.

The mechanical architecture of the proposed injection-molding device is designed to fulfill three primary functions: supporting the injection unit while enabling linear positional adjustment for molds of different sizes; supporting the filament spool without restricting feed motion during extrusion; and immobilizing the mold throughout filling. Based on these requirements, the architecture is organized into three main subsystems: arm, mold clamp, and base (Figure 6).

The arm is configured as an inverted L-shaped member that elevates the injection unit and transmits its load to the base. Its horizontal segment is modeled as a cantilever under bending. A preliminary geometric envelope is established based on the target manufacturing range, with a vertical reach of 45 cm and a horizontal length of 25 cm, using the typical part-size scale reported for fused deposition modeling systems [44].

The initial cross-sectional sizing follows elementary bending theory, $\sigma = Mc/I$, using an allowable stress of 240 MPa for Al 6061, load moment derived from a 2.5 kg injection-unit mass, and a square section assumption [45], [46]. This first-pass calculation yields a minimum side dimension of approximately 0.5 cm. Since this value is structurally sufficient but not adequate for assembly and alignment constraints, final sizing is governed by integration requirements of the sliding plate and by the required vertical alignment between nozzle and mold fastener, resulting in a practical arm section of 12×7cm (Figures 6 and 7).

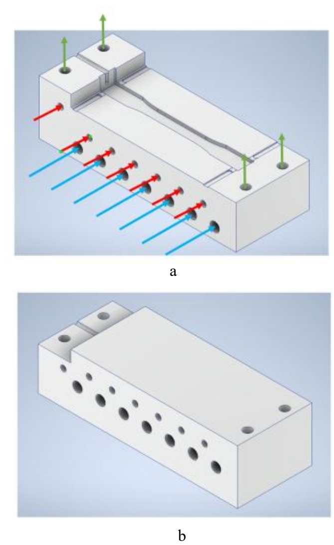

Fig. 5 Preliminary mold design integrating thermal-management and fastening features for the tensile-specimen cavity. (a) First mold half showing the proposed layout of cartridge heater bores (red arrows), cooling channels (blue arrows), and fastener positions (green arrows). (b) Second mold half

showing the corresponding channel network and bolt interfaces for mold closure and thermal operation.

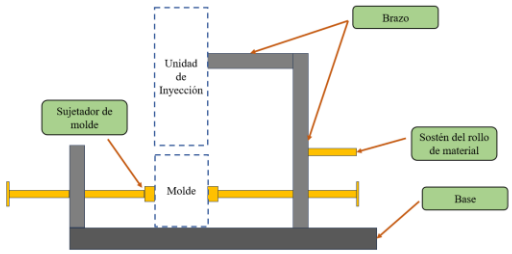

Fig. 6 Conceptual structural layout of the proposed injection-molding device.

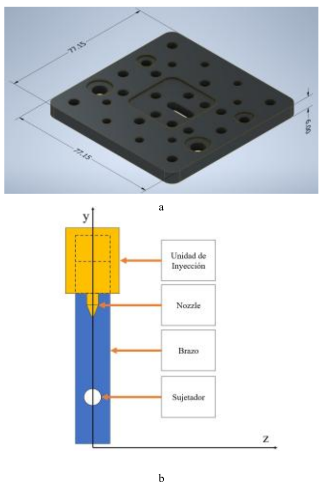

Fig. 7 Integration geometry for the injection-unit support system. (a) Dimensions of the injection-unit sliding plate. (b) Conceptual front-view alignment of the injection unit, nozzle, arm, and mold fastener along the y–z reference axes.

Mold fixation is implemented with threaded C-clamp elements mounted on both sides of the mold to apply controllable compression and maintain positional stability during filling. The base is defined as a flat platform that integrates and supports all subsystems. The resulting conceptual assembly consolidates the minimum functional elements required for stable operation of the molding device (Figure 8).

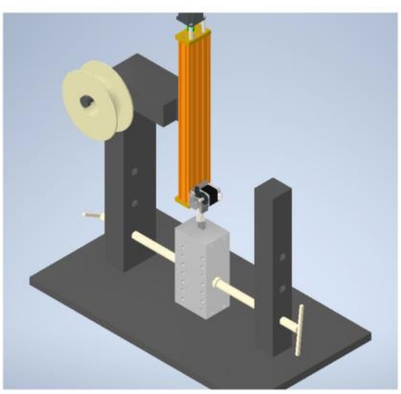

Fig. 8 Final conceptual design of the filament-extrusion-driven injection molding device. The assembly integrates a structural base, support columns, a vertical positioning system for the injection unit, a filament spool holder, a nozzle aligned with the mold inlet, and a laterally clamped mold module.

IV. Conclusions and Practical Implications

The results delineate a relatively narrow, though internally coherent, operating window for the proposed low-cost, extrusion-driven injection concept. As shown in Figure 3, the hot-end pressure response remains relatively stable across the evaluated thermal range, with an outlet pressure near 7.7 MPa and only modest variation between 493 and 533 K. At a selected operating point of 32.56 mm³/s, the estimated filling time is approximately 258 s. While this minute-scale filling regime suggests technical feasibility for controlled specimen fabrication, it simultaneously underscores the salience of thermal losses and melt solidification as primary design constraints. It is important to acknowledge that these findings are contingent upon the specific operating conditions evaluated herein.

Within this operating window, the geometry study depicted in Figure 4 appears to support selecting the constant-cylindrical sprue as the preferred baseline configuration for the ASTM D638 Type I cavity. The cylindrical sprue yields marginally higher final quality than the tapered alternative at the evaluated extremes, 99.72% versus 99.56% at a 34 mm runner length, and 99.36% versus 99.32% at 5 mm. Sink-depth behavior also appears to favor the cylindrical option within the practical range, remaining near 0.01 mm from 5 to 30 mm and increasing only at the longest-runner condition. Deflection trends offer additional support for this assessment, as the tapered sprue exhibits higher values and thus comparatively reduced dimensional robustness. Nevertheless, the quantitative differences should be interpreted with caution, as they are modest in absolute terms.

The principal trade-off observed is volumetric contraction, which increases with runner length and is generally greater for the cylindrical sprue, reaching approximately 5.06% within the evaluated set. Nonetheless, the disparity between sprue types remains below 5% and, given the observed improvements in quality, sink control, and deflection stability, may be considered relatively minor. Spatial mapping further corroborates this interpretation: contraction is distributed throughout the specimen, while sink marks are localized near the sprue-entry transition. Accordingly, the selected geometry appears to enhance overall specimen quality while maintaining low and spatially confined local defect severity. It is prudent, however, to reiterate that these conclusions are context-dependent and may warrant further experimental validation.

From a system design perspective, the present study suggests that mold material selection, vent geometry, heating layout, optional cooling strategy, and structural alignment are strongly interdependent. The principal contribution is not the identification of a single optimized parameter but the articulation of a reproducible design methodology that links functional requirements to first-order mechanical, thermal, and process constraints prior to hardware fabrication. This approach is arguably most relevant for early-stage engineering development, where minimizing uncertainty prior to prototyping is paramount. Nonetheless, further research is advised to evaluate the generalizability of these methodological recommendations.

The low-cost rationale is further contextualized by reference to production-class guidelines. While SPI guidance prescribes very high cycle counts, the present concept is scoped for approximately 1000 parts. Consequently, the intended use case is not industrial high-throughput molding but for comparative testing, laboratory prototyping, and educational deployment, in which acceptable repeatability is prioritized. Thus, extended cycle times may be justified if they ease accessibility, reduce entry cost, and promote design transparency. These trade-offs should be evaluated in light of the application's specific objectives and constraints.

The initial requirement-driven strategy is completed in this study through a closed decision sequence: (i) definition of the target use case and standardized cavity, (ii) establishment of a feasible process operating window, (iii) comparative assessment of sprue and runner effects on quality and defect metrics, and (iv) integration of venting, thermal, and structural constraints into a single conceptual architecture. Within this sequence, the constant cylindrical sprue was selected as the baseline configuration because it offers the best overall balance between surface quality, sink-depth robustness, and deflection stability, while incurring an acceptable contraction penalty under low-throughput operation. This closes the proposed design methodology as a reproducible pre-prototyping framework for laboratory-scale comparative molding.

G.1. Conclusions

1. Technical feasibility has been demonstrated, within the scope of this study, for low-volume manufacturing of standardized tensile specimens under the evaluated operating conditions. It is, however, essential to acknowledge that these results may not be directly generalizable to broader manufacturing contexts without further empirical validation.

2. The constant-cylindrical sprue is identified as the optimal geometry in this context, as it appears to improve surface quality and defect robustness, notwithstanding a modest contraction penalty. Nevertheless, the optimality of this configuration may depend on the specific parameters and constraints examined herein.

3. Cycle time remains the principal limitation, as minute-scale filling amplifies sensitivity to thermal management and melt-flow stability. This constraint should be carefully weighed in subsequent design iterations.

4. This study advances a transferable pre-prototyping framework that integrates venting, thermal design, structural considerations, and process calculations into a unified, requirement-driven workflow. The applicability of this framework to alternate contexts or scales, however, remains to be established.

G.2. Practical Implications

In laboratory and instructional contexts, this framework provides a practical approach to implementing low-cost comparative molding for small-batch specimen production, material screening, and teaching applications. The current configuration is intended for repeatable low-volume operation, not industrial throughput, and should be interpreted within its stated methodological assumptions.

From a design perspective, the results indicate that sprue and runner choices should be treated as a coupled multi-objective problem. Under low-throughput conditions, prioritizing surface quality, sink-mark control, and deflection stability is more consequential than marginal reductions in volumetric contraction.

The immediate next step is experimental validation. Priority tasks include monitoring instrumented-cavity pressure and temperature, quantitative repeatability assessment, and iterative optimization of heater placement and cooling-channel layout to reduce cycle time while preserving dimensional stability and defect control.

Acknowledgments

The authors express their gratitude to the Research Group in Design, Manufacturing, and Materials (DM + M) at the Technological University of Panama (https://utp.ac.pa/, accessed on 28 January 2026), National Research System (SNI), and the Centro de Estudios Multidisciplinarios en Ciencia, Ingeniería y Tecnología (CEMCIT-AIP). This research was funded by the Panamanian Bureau of Science, Technology, and Innovation (Secretaría Nacional de Ciencia, Tecnología e Innovación, SENACYT) under grant FIED22-13.

References

[1] Y. Qiao, L. D. Fring, M. R. Pallaka, et K. L. Simmons, « A review of the fabrication methods and mechanical behavior of continuous thermoplastic polymer fiber–thermoplastic polymer matrix composites », *Polymer Composites*, vol. 44, nº 2, p. 694-733, févr. 2023, doi: 10.1002/pc.27139.

[2] F. Ozturk, M. Cobanoglu, et R. E. Ece, « Recent advancements in thermoplastic composite materials in aerospace industry », *Journal of Thermoplastic Composite Materials*, vol. 37, nº 9, p. 3084-3116, sept. 2024, doi: 10.1177/08927057231222820.

[3] J. M. Chacón, M. A. Caminero, P. J. Núñez, E. García-Plaza, I. García-Moreno, et J. M. Reverte, « Additive manufacturing of continuous fibre reinforced thermoplastic composites using fused deposition modelling: Effect of process parameters on mechanical properties », *Composites Science and Technology*, vol. 181, p. 107688, sept. 2019, doi: 10.1016/j.compscitech.2019.107688.

[4] X. Xu, H. Ren, S. Chen, X. Luo, F. Zhao, et Y. Xiong, « Review on melt flow simulations for thermoplastics and their fiber reinforced composites in fused deposition modeling », *Journal of Manufacturing Processes*, vol. 92, p. 272-286, 2023, doi: 10.1016/j.jmapro.2023.02.039.

[5] L. Yan et H. Xu, « Lightweight composite materials in automotive engineering: State-of-the-art and future trends », *Alexandria Engineering Journal*, vol. 118, p. 1-10, avr. 2025, doi: 10.1016/j.aej.2024.12.002.

[6] F. Ozturk, M. Cobanoglu, et R. E. Ece, « Recent advancements in thermoplastic composite materials in aerospace industry », *Journal of Thermoplastic Composite Materials*, vol. 37, nº 9, p. 3084-3116, sept. 2024, doi: 10.1177/08927057231222820.

[7] R. Phiri, S. M. Rangappa, S. Siengchin, O. P. Oladijo, et T. Ozbakkaloglu, « Advances in lightweight composite structures and manufacturing technologies: A comprehensive review », *Heliyon*, vol. 10, nº 21, nov. 2024, doi: 10.1016/j.heliyon.2024.e39661.

[8] M. Fernandez-Vicente, W. Calle, S. Ferrandiz, et A. Conejero, « Effect of Infill Parameters on Tensile Mechanical Behavior in Desktop 3D

Printing », *3D Printing and Additive Manufacturing*, vol. 3, nº 3, p. 183-192, sept. 2016, doi: 10.1089/3dp.2015.0036.
[9] J. Khatwani et V. Srivastava, « Effect of Process Parameters on Mechanical Properties of Solidified PLA Parts Fabricated by 3D Printing Process », in *3D Printing and Additive Manufacturing Technologies*, L. J. Kumar, P. M. Pandey, et D. I. Wimpenny, Éd., Singapore: Springer Singapore, 2019, p. 95-104. doi: 10.1007/978-981-13-0305-0_9.
[10] A. Pulipaka, K. M. Gide, A. Beheshti, et Z. S. Bagheri, « Effect of 3D printing process parameters on surface and mechanical properties of FFF-printed PEEK », *Journal of Manufacturing Processes*, vol. 85, p. 368-386, janv. 2023, doi: 10.1016/j.jmapro.2022.11.057.
[11] A. K. Sood, R. K. Ohdar, et S. S. Mahapatra, « Parametric appraisal of mechanical property of fused deposition modelling processed parts », *Materials & Design*, vol. 31, nº 1, p. 287-295, janv. 2010, doi: 10.1016/j.matdes.2009.06.016.
[12] A. Lepoivre, N. Boyard, A. Levy, et V. Sobotka, « Methodology to assess interlayer quality in the material extrusion process: A temperature and adhesion prediction on a high performance polymer », *Additive Manufacturing*, vol. 60, p. 103167, déc. 2022, doi: 10.1016/j.addma.2022.103167.
[13] C. G. Amza, A. Zapciu, G. Constantin, F. Baciu, et M. I. Vasile, « Enhancing Mechanical Properties of Polymer 3D Printed Parts », *Polymers*, vol. 13, nº 4, p. 562, févr. 2021, doi: 10.3390/polym13040562.
[14] Y. P. Shaik, J. Schuster, H. R. Katherapalli, et A. Shaik, « 3D Printing under High Ambient Pressures and Improvement of Mechanical Properties of Printed Parts », *J. Compos. Sci.*, vol. 6, nº 1, p. 16, janv. 2022, doi: 10.3390/jcs6010016.
[15] J. Ghorbani, P. Koirala, Y.-L. Shen, et M. Tehrani, « Eliminating voids and reducing mechanical anisotropy in fused filament fabrication parts by adjusting the filament extrusion rate », *Journal of Manufacturing Processes*, vol. 80, p. 651-658, août 2022, doi: 10.1016/j.jmapro.2022.06.026.
[16] A. Ramalho, D. Freitas, et H. Almeida, « The anisotropy and friction effect in the design of 3D printed PLA parts – A case study », *Materials Today: Proceedings*, août 2023, doi: 10.1016/j.matpr.2023.08.196.
[17] C. Savandaiah, J. Maurer, B. Plank, G. Steinbichler, et J. Sapkota, « Rapid consolidation of 3D printed composite parts using compression moulding for improved thermo mechanical properties », *RPJ*, vol. 28, nº 10, p. 1943-1955, oct. 2022, doi: 10.1108/RPJ-11-2021-0311.
[18] L. B. Said, B. Ayadi, S. Alharbi, et F. Dammak, « Recent Advances in Additive Manufacturing: A Review of Current Developments and Future Directions », *Machines*, vol. 13, nº 9, sept. 2025, doi: 10.3390/machines13090813.
[19] A. Patti, « Challenges to Improve Extrusion-Based Additive Manufacturing Process of Thermoplastics toward Sustainable Development », *Macromolecular Rapid Communications*, vol. 45, nº 17, p. 2400249, 2024, doi: 10.1002/marc.202400249.
[20] D. Kazmer, A. M. Peterson, D. Masato, A. R. Colon, et J. Krantz, « Strategic cost and sustainability analyses of injection molding and material extrusion additive manufacturing », *Polymer Engineering & Sci*, vol. 63, nº 3, p. 943-958, mars 2023, doi: 10.1002/pen.26256.
[21] B. Sztorch, D. Brząkalski, M. Jałbrzykowski, et R. E. Przekop, « Processing Technologies for Crisis Response on the Example of COVID-19 Pandemic—Injection Molding and FFF Case Study », *Processes*, vol. 9, nº 5, p. 791, avr. 2021, doi: 10.3390/pr9050791.
[22] A. B. Lozano, S. H. Álvarez, C. V. Isaza, et W. Montealegre-Rubio, « Analysis and Advances in Additive Manufacturing as a New Technology to Make Polymer Injection Molds for World-Class Production Systems », *Polymers*, vol. 14, nº 9, p. 1646, avr. 2022, doi: 10.3390/polym14091646.
[23] S. B. Rocha, T. Zhiltsova, V. Neto, et M. S. A. Oliveira, « Optimization to Assist Design and Analysis of Temperature Control Strategies for Injection Molding—A Review », *Materials*, vol. 15, nº 12, p. 4048, juin 2022, doi: 10.3390/ma15124048.
[24] O. Ogorodnyk et K. Martinsen, « Monitoring and Control for Thermoplastics Injection Molding A Review », *Procedia CIRP*, vol. 67, p. 380-385, 2018, doi: 10.1016/j.procir.2017.12.229.
[25] R. Wick-Joliat, M. Schroffenegger, et D. Penner, « Multi-material ceramic material extrusion 3D printing with granulated injection molding feedstocks », *Ceramics International*, vol. 49, nº 4, p. 6361-6367, févr. 2023, doi: 10.1016/j.ceramint.2022.10.170.
[26] A. M. Gohn, D. Brown, G. Mendis, S. Forster, N. Rudd, et M. Giles, « Mold inserts for injection molding prototype applications fabricated via material extrusion additive manufacturing », *Additive Manufacturing*, vol. 51, p. 102595, mars 2022, doi: 10.1016/j.addma.2022.102595.
[27] A. Benitez-Lozano, C. Vargas-Isaza, et W. Montealegre-Rubio, « Development, Simulation of Temperatures, and Experimentation in Injection Molds Obtained through Additive Manufacturing with Photocurable Polymeric Resins », *Polymers*, vol. 15, nº 5, p. 1071, févr. 2023, doi: 10.3390/polym15051071.
[28] D20 Committee, « Test Method for Tensile Properties of Plastics », ASTM International, 2022. doi: 10.1520/D0638-14.
[29] M. J. Prajapati, A. Kumar, S.-C. Lin, et J.-Y. Jeng, « Closed-cell metamaterial composites 3D printed with hybrid FFF process for tunable mechanical and functional properties », *Thin-Walled Structures*, vol. 192, p. 111168, nov. 2023, doi: 10.1016/j.tws.2023.111168.
[30] R. Zou *et al.*, « Isotropic and anisotropic elasticity and yielding of 3D printed material », *Composites Part B: Engineering*, vol. 99, p. 506-513, août 2016, doi: 10.1016/j.compositesb.2016.06.009.
[31] Jiangzhi, « Injection Pressure in Injection Molding : You Essential Need to Know1 ». Consulté le: 14 février 2026. [En ligne]. Disponible sur: https://www.swcpu.com/blog/injection-pressure-in-injection-molding/
[32] iDig 3DPrinting, « TABLE OF 3D PRINTER FILAMENT SPOOL DIMENSIONS ». [En ligne]. Disponible sur: https://www.idig3dprinting.co.uk/news/how-to-guides/3d-printer-filament-spool-sizes/
[33] LANXESS Energizing Chemistry, « Part and Mold Design Guide ». 2007. [En ligne]. Disponible sur: https://techcenter.lanxess.com/scp/americas/en/docguard/Part_and_Mold_Design_Guide.pdf?docId=77015
[34] DME Company, « Mold Components Catalog ». [En ligne]. Disponible sur: https://online.flippingbook.com/view/668526/
[35] M. Enriconi *et al.*, « A Comprehensive Review of Fused Filament Fabrication: Numerical Modeling Approaches and Emerging Trends », *Applied Sciences*, vol. 15, nº 12, juin 2025, doi: 10.3390/app15126696.
[36] D. Acierno et A. Patti, « Fused Deposition Modelling (FDM) of Thermoplastic-Based Filaments: Process and Rheological Properties—An Overview », *Materials (Basel)*, vol. 16, nº 24, p. 7664, déc. 2023, doi: 10.3390/ma16247664.
[37] F. Czerwinski, « Thermal Stability of Aluminum Alloys », *Materials*, vol. 13, nº 15, p. 3441, août 2020, doi: 10.3390/ma13153441.
[38] G. Hantke, « Injection molding parameters: The key to high quality and efficiency », assemblean. Consulté le: 14 février 2026. [En ligne]. Disponible sur: https://assemblean.com/en/blog/injection-molding-parameters-the-key-to-high-quality-and-efficiency/
[39] Jason, « A Simple Guide to Cycle Time For Injection Molding », Protoshop Inc. Consulté le: 14 février 2026. [En ligne]. Disponible sur: https://protoshopinc.com/blog/a-simple-guide-to-cycle-time-in-plastic-injection-molding/
[40] Plásticos Lezo, « Fill Time in Injection Molding: Importance and Optimization ». Consulté le: 14 février 2026. [En ligne]. Disponible sur: https://plasticoslezo.com/en/dictionary/fill-time-injection-molding/?utm_source=chatgpt.com
[41] D. Kazmer, *Injection mold design engineering*, 2nd edition. Munich : Cincinnati : Munich: Hanser Publications, ; Hanser Publishers, 2016.
[42] K. Suhas, « Determining Vent Depths in Injection Molding ». [En ligne]. Disponible sur: https://www.ptonline.com/articles/determining-vent-depths-in-injection-molding
[43] WATTCO, « CALENTADORES DE CARTUCHO ». [En ligne]. Disponible sur: https://www.wattco.com/es/product_category/calentadores-de-cartucho/#:~:text=Los%20calentadores%20de%20cartucho%20alcanzar%C3%A1n,nuestro%20cat%C3%A1logo%2C%20p%C3%A1gina%207.2).
[44] W. Stone, « How Big can a 3D Printer Print? », Printing Spot. [En ligne]. Disponible sur: https://www.3dprintingspot.com/post/how-big-can-a-3d-printer-print
[45] F. P. Beer, *Mecánica de materiales*, 6a ed. México, D.F.: McGraw-Hill Interamericana, 2013.
[46] R. G. Budynas et J. E. Shigley, *Diseño en ingeniería mecánica de Shigley*, 8a ed. México, D.F.: McGraw-Gill Interamericana, 2008.